Distribution- Versus Correlation-Induced Anomalous Transport in Quenched Random Velocity Fields

Marco Dentz
Spanish National Research Council (IDÆA-CSIC), Barcelona, Spain

Diogo Bolster
Environmental Fluid Dynamics Laboratory, University of Notre Dame, Indiana, USA
(Received 6 August 2010)

We study mechanisms of anomalous transport in quenched random media. Broad disorder point distributions and strong disorder correlations cause anomalous transport and can lead to the same anomalous scaling laws for the mean and variance of the particle displacements. The respective mechanisms, however, are fundamentally different. This difference is reflected in the spatial particle densities and first passage time distributions, which provide an indicator to identify the origins of anomalous transport.

DOI: PACS numbers: 46.65.+g, 05.40.−a, 47.56.+r

Transport in disordered media is in general anomalous in the sense that the average behavior is non-Markovian [1]. Anomalous transport can manifest itself as nonlinear scaling of the mean and the variance of particle displacements, tails of the spatial particle densities and the first passage time distributions [2,3]. Such behavior has been ubiquitously found for particle movements in quenched random environments including porous media [4–7], gels [8], optical media [9] and crowded environments such as living cells [10–12]. The observed anomalous diffusive behavior has been modeled using Lévy flights and walks, continuous time random walks (e.g., Refs. [2,3,13], and references therein), projector formalisms [1,14], fractional Brownian motion [15] and nonstationary Gaussian noise [16], among others. As highlighted in Refs. [10–12,15], the origin of anomalous transport is often unknown and thus it is not always clear, which model of anomalous transport is applicable. In this Letter, we address this question by studying the different manifestations of anomalous transport as induced by strong (power-law) disorder correlation and broad disorder point distributions (power-law tails towards extreme values).

Particle movement in a random medium can be described by the nonlinear Langevin equation [e.g., [17]]

$$dx(t) = v[x(t)]dt + \sqrt{2D\{v[x(t)]\}dt}\,\xi(t), \qquad (1)$$

where we employ the Ito interpretation. The drift $v(x) > 0$ is a quenched random field with nonzero mean, $D[v(x)]$ a drift-dependent diffusion coefficient and $\xi(t)$ a Gaussian random variable characterized by zero mean and unit variance. The initial condition is $x(t = 0) = x_0$. The particle density $c(x, t) = \langle \delta[x - x(t)] \rangle$ satisfies the Fokker-Planck equation

$$\frac{\partial c(x, t)}{\partial t} + \frac{\partial}{\partial x} v(x) c(x, t) - \frac{\partial^2}{\partial x^2} D[v(x)] c(x, t) = 0. \qquad (2)$$

Disorder model.—We consider a spatial disorder organization in bins of varying sizes with constant drift within a given bin. The random velocity $v(x)$ then is represented by $v(x) = \sum_{m=-\infty}^{\infty} v_m \mathbf{I}_{B_m}$ with $B_m = \{x | a_m < x \le a_{m+1}\}$. The indicator function $\mathbf{I}_{B_m}(x)$ is one if $x \in B_m$ and zero otherwise. The a_m are given by $a_m = -l_0 + \sum_{i=1}^{m} l_i$ and $a_{-m} = -\sum_{i=0}^{m} l_{-i}$ with $m \ge 0$. Length l_i and velocity v_m are independent identically distributed positive random numbers, whose distributions are $p_l(l)$ and $p_v(v)$, respectively. The random velocity field $v(x)$ is stationary and ergodic. The mean velocity is $\bar{v} \neq 0$, with the overbar denoting the ensemble average. The velocity correlation is $C(x - x') = \overline{\nu(x)\nu(x')}/\sigma_v^2$, with $\nu(x)$ the velocity fluctuation and σ_v^2 the velocity variance. If mean or variance of $p_v(v)$ do not exist we define them by introducing a filter such that $\bar{v} = -d/d\lambda \ln[\hat{p}_v(\lambda)]_{\lambda=\lambda_c}$ and $\sigma_v^2 = -d^2/d\lambda^2 \ln[\hat{p}_v(\lambda)]_{\lambda=\lambda_c}$ with cutoff mode λ_c. The hat denotes the Laplace transform and λ is the Laplace variable. The correlation function of $v(x)$ is given by

$$C(x) = \int_0^\infty dl\, p_l(l) \max(1 - |x|/l, 0). \qquad (3)$$

A power-law distribution $p_l(l) \propto l^{-1-\gamma}$ results in the power-law correlation function $C(x) \propto |x|^{-\gamma}$ for large distance. For a constant bin size [i.e., $p_l(l) = \delta(l - l_0)$], the velocity field is delta-correlated, $C(x) = l_0 \delta(x)$, at an observation scale much larger than l_0.

Average transport.—We present a systematic upscaling procedure that provides an explicit link between the statistics of the microscale disorder model and the average transport behavior. This approach includes the following steps: (i) increase the dimensionality of the original Langevin equation by introducing an operational time; (ii) coarse grain the resulting set of equations respecting the spatial disorder organization; (iii) ensemble average of the single realization particle density.

Defining "operational" time s by $dt = v_c v[x(s)]^{-1} ds$ with v_c a characteristic drift,(1) can be written as

$$dx(s) = v_c ds + \sqrt{2D\{v[x(s)]\} v_c v[x(s)]^{-1} ds}\,\xi(s), \quad (4a)$$

$$dt(s) = v_c v[x(s)]^{-1} ds. \quad (4b)$$

We coarse grain (4a) so that the spatial transition is equal to the length of a bin for each random walk step. This implies that the drift is constant during a step, and it guarantees that at subsequent steps particle velocities are independent. We denote $v(x_n) = v_n$. Thus, the spatial increment of the coarse-grained random walk is $x_{n+1} - x_n = \ell_n$ with ℓ_n the bin length at position x_n. The operational time increment $\sigma_n = s_{n+1} - s_n$ needed to traverse distance ℓ_n is the first arrival time for the biased random walk (4a) over the distance ℓ_n and thus a random variable. The distribution of σ_n is denoted by $p_\sigma(\sigma_n|l_n, v_n)$. The mean of σ_n is ℓ_n/v_c and its variance is $2\epsilon_n \ell_n^2/v_c^2$ with $\epsilon_n = D(v_n)/(\ell_n v_n)$. In the limit $\epsilon_n \ll 1$, the distribution of σ_n can be approximated by $p_\sigma(\sigma_n|l_n, v_n) = \delta(\sigma_n - \ell_n/v_c)$. With these discretizations, Eq. (4) becomes

$$x_{n+1} = x_n + \ell_n, \qquad t_{n+1} = t_n + \tau_n, \quad (5)$$

where $\tau_n \equiv \sigma_n v_c / v_n$. Note that the transition times τ_n depend on the specific disorder configuration, which reflects the quenched nature of the random field $v(x)$.

In order to perform the ensemble average, we have to express the single realization particle density $c(x, t)$ in terms of the coarse-grained particle position x_n. To this end, we note that the number of steps needed to reach a certain time t is quantified by the renewal process $n_t = \sup(n|t_n \le t)$ and, accordingly, x_{n_t} is the particle location at time $t_{n_t} \le t$. The actual particle position $x(t)$ at time t is given by linear interpolation such that $x(t) = x_{n_t} + \ell_{n_t}(t - t_{n_t})/\tau_{n_t}$. Thus, the single realization particle density $c(x, t)$, in terms of the coarse-grained space-time particle trajectory, is (5) as $c(x, t) = \langle \delta[x - x_{n_t} - \ell_{n_t}(t - t_{n_t})/\tau_{n_t}]\rangle$, where the angular brackets (noise average) now denote the average over σ_n. Inserting a Kronecker delta gives $c(x, t) = \sum_{n=0}^{\infty} \langle \delta[x - x_n - \ell_n(t - t_n)/\tau_n]\delta_{n,n_t}\rangle$. Noting that $n = n_t$ is equivalent to $0 \le t - t_n < \tau_n$, this expression can be written as

$$c(x, t) = \sum_{n=0}^{\infty} \langle \delta[x - x_n - \ell_n(t - t_n)/\tau_n] \mathbf{I}_{A_n}(t - t_n)\rangle, \quad (6)$$

where $A_n = \{t|0 \le t < \tau_n\}$. Introducing two Dirac deltas in (6) and taking the ensemble average gives

$$\bar{c}(x, t) = \int_0^t dt' \int dx' \sum_{n=0}^{\infty} \overline{\langle \delta(x' - x_n)\delta(t' - t_n)\rangle} \times \overline{\langle \delta[x - x' - \ell_n(t - t')/\tau_n] \mathbf{I}_{A_n}(t - t')\rangle}. \quad (7)$$

The ensemble average can be spit because the ℓ_n and τ_n at subsequent steps are not correlated by definition. Performing the second average explicitly, the mean particle density is given by

$$\bar{c}(x, t) = \int_0^t dt' \int dx' \sum_{n=0}^{\infty} P_n(x', t') \int_{t-t'}^{\infty} d\tau \times \int_0^{\infty} d\ell\, \delta[x - x' - \ell(t - t')/\tau]\psi(\ell, \tau), \quad (8)$$

with $P_n(x, t) = \overline{\delta(x - x_n)\langle\delta(t - t_n)\rangle}$ and the joint transition length and time distribution defined as

$$\psi(\ell, \tau) = \frac{v_c p_l(\ell)}{\tau^2} \int_0^{\infty} d\sigma \sigma p_\sigma(\sigma|\ell, v_c\sigma/\tau) p_v(v_c\sigma/\tau). \quad (9)$$

We denote the ith spatial moment of $\psi(x, t)$ by $\mu_i(t)$. The space-time particle density $P_n(x, t)$, satisfies

$$P_{n+1}(x, t) = \int dx' \int_0^t dt' P_n(x', t')\psi(x - x', t - t'). \quad (10)$$

Eqs. (8) and (10) describe the particle density of a fully coupled CTRW (e.g., [18]) whose space-time trajectory is given by Eq. (5), with τ_n and ℓ_n at each step drawn from $\psi(\ell, \tau)$.

Anomalous transport can be characterized in terms of the first passage time distribution and the time evolution of the mean and variance of the particle displacements. The distribution of the first passage time $t_f(x)$ of a particle injected at x_0 at time $t = 0$, is defined by $\bar{f}(t, x) = \overline{\langle\delta[t - t_f(x)]\rangle}$. An explicit expression for $\bar{f}(t, x)$ can be derived by using a similar reasoning as above for the derivation of the average particle density $\bar{c}(x, t)$. From (8) and (10) we obtain explicit Laplace space expressions for the mean and mean squared displacements $m_1(t) = \overline{\langle x(t)\rangle}$ and $m_2(t) = \overline{\langle x(t)^2\rangle}$,

$$\hat{m}_1(\lambda) = \int_0^{\lambda} d\lambda' \frac{\hat{\mu}_1(\lambda')}{\lambda^2[1 - \hat{\mu}_0(\lambda)]}, \quad (11)$$

$$\hat{m}_2(\lambda) = \int_0^{\lambda} d\lambda' \frac{2\lambda'\hat{\mu}_2(\lambda')}{\lambda^3[1 - \hat{\mu}_0(\lambda)]} + \frac{2\hat{\mu}_1(\lambda)\hat{m}_1(\lambda)}{[1 - \hat{\mu}_0(\lambda)]}. \quad (12)$$

The variance $\kappa(t) = m_2(t) - m_1(t)^2$ measures the width of the mean particle distribution.

The average transport model in 1 (8)–(10) allows the systematic study of anomalous average transport induced by (i) disorder point distributions and (ii) disorder correlations. For illustration, we choose $D[v(x)] = \mathcal{D}v(x)/v_c$ so that $\epsilon_n = \mathcal{D}/(\ell_n v_c)$. Furthermore, we consider scenarios for which $\epsilon_n \ll 1$ for almost all n and approximate the joint transition length and time distribution by $\psi(\ell, \tau) = (v_c/\ell)p_l(\ell)p_\theta(\tau v_c/\ell)$.

Distribution-induced anomalous diffusion.—First, let us consider the scenario of a delta distribution of bin length $p_l(l) = \delta(l - l_0)$. The latter implies $C(x) = l_0\delta(x)$ for an observation scale $L \gg l_0$. Average transport for this scenario follows a decoupled CTRW. This transport behavior

2

has been well studied in the literature [3,13,18–20]. Anomalous diffusion here is caused by a power-law distribution of transition times $\mu_0(t) \propto t^{-1-\beta}$, which arises for the velocity distribution $p_v(v) \propto v^{\beta-1}/(1+v/v_c)^{1+\beta}$. In fact, all moments scale as $\mu_i(t) \propto t^{-1-\beta}$. A typical realization of this disorder model for $\beta = 3/2$ is illustrated by

where the gray scales indicate different values of $v(x)$. In the computational examples, we refer to this specific scenario as *case 1*.

Anomalous transport here is distribution dominated because the quenched random field is essentially uncorrelated. The first moment of the particle distribution asymptotically goes like $m_1(t) \propto t^{\beta}$ for $0 < \beta < 1$ and $m_1(t) \propto t$ for $\beta > 1$. Similarly, the variance evolves asymptotically as $\kappa(t) \propto t^{2\beta}$ for $0 < \beta < 1$ and as $\kappa(t) \propto t^{3-\beta}$ for $1 < \beta < 2$. For $0 < \beta < 2$ diffusion is anomalous, while for $\beta > 2$, transport is asymptotically normal and $\kappa(t) \propto t$. The behavior of $\kappa(t)$ is illustrated in Fig. 1 for $\beta = 3/2$. The first passage time distribution scales as $\bar{f}(t, x) \propto t^{-1-\beta}$ for $0 < \beta < 2$.

Correlation-induced anomalous diffusion.—Next, we consider a power-law distribution of bin sizes, $p_l(l) \propto l^{-1-\gamma}$, which leads to a power-law correlation function $C(x) \propto |x|^{-\gamma}$. We consider velocity distributions $p_v(v)$ that go to zero exponentially fast for small v. This means transport is not limited by slow velocities as in the previous case. Anomalous transport here is correlation-induced.

For illustration, we choose a power-law distribution $p(v) \propto v^{-2}\exp(-v_c/v)$ and a lognormal velocity distribution. A typical realization of the power-law $p_v(v)$ for $\gamma = 3/2$ is given by

to which we refer in the following as *case 2*. A typical realization of the lognormal $p(v)$ and $\gamma = 3/4$ is illustrated by

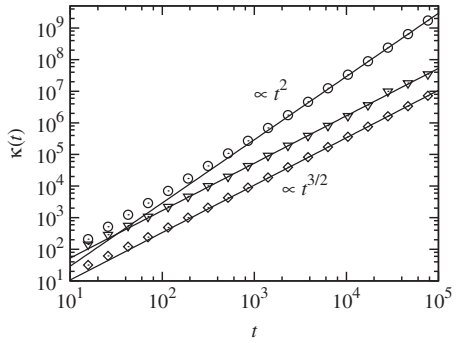

FIG. 1. Time behavior of the spatial variance of the mean particle distributions for (rectangles) case 1, (triangles) case 2, and (circles) case 3. The solid lines indicate the asymptotic behavior. The results are obtained by Monte Carlo simulations based on (5) for 10^5–10^6 disorder realizations.

which is referred to as *case 3* in the computational examples.

At late times, the moments $\mu_i(t)$ of $\psi(x, t)$ scale as

$$\mu_i(t) \propto t^{i-1-\gamma} \int_0^\infty dv v^{i-\gamma} p_v(v). \tag{13}$$

Note that in contrast to the distribution dominated scenario, the scaling behavior here depends on the order of the moment. The mean and mean squared particle displacements (11) and (12) exist only if moments $\mu_1(t)$ and $\mu_2(t)$ in (13) exist. If the velocity distribution is tailed towards high velocities, the mean and mean squared particle displacements may diverge. In this case, the behavior is Levy flight-like, characterized by high velocities that can persist over long distances. This can be observed for the power-law velocity distribution, for which $\mu_2(t)$ diverges logarithmically for $0 < \gamma < 1$. If $\mu_i(t) < \infty$ for $i = 1, 2$, the long time behavior of the $m_1(t)$ and $m_2(t)$ can be obtained by inserting the Laplace transforms of (13) into (11) and (12), expansion for small λ and using Tauberian theorems. We find that the centroid of the particle distribution behaves asymptotically as $m_1(t) \propto t$. The variance scales as $\kappa(t) \propto t^2$ for $0 < \gamma < 1$, that is, diffusion is ballistic. For $1 < \gamma < 2$, the variance behaves as $\kappa(t) \propto t^{3-\gamma}$. For $\gamma > 2$ transport is asymptotically normal. This behavior has been obtained in a different context in Refs. [21,22].

Distribution versus correlation-induced behavior.—Figure 1 illustrates the spatial variance $\kappa(t)$ for cases 1–3 obtained from Monte Carlo simulations and the predicted anomalous scaling behavior. The ballistic behavior of $\kappa(t)$ for $0 < \gamma < 1$ (case 3) is due the fact that the same velocities can persist over relatively long distances. The displacement variance is then dominated by the velocity differences in the long conduits, which gives rise to the t^2 scaling of $\kappa(t)$. The variance $\kappa(t)$ for $1 < \gamma < 2$ (case 2) scales the same way as its counterpart in the distribution dominated scenario for $1 < \beta < 2$ (case 1). However, the mechanisms leading to this behavior are fundamentally

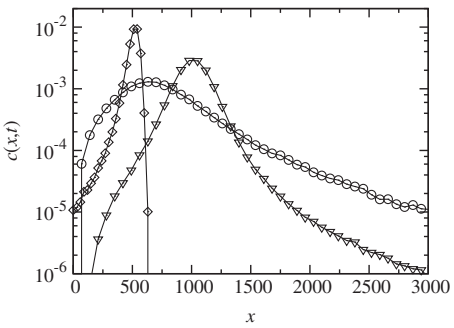

FIG. 2. Particle density $\bar{c}(x, t)$ for (rectangles) case 1, (triangles) case 2, and (circles) case 3 at $t = 10^3$. The results are obtained by Monte Carlo simulations based on (5) for 10^6–10^7 disorder realizations.

3

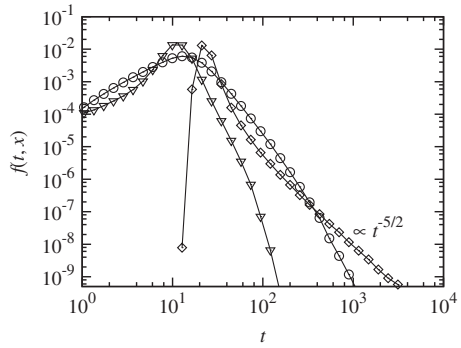

FIG. 3. First passage time distributions for (rectangles) case 1, (triangles) case 2, and (circles) case 3. The results are obtained by Monte Carlo simulations based on (5) for 10^7 disorder realizations. Particles are injected instantaneously at time $t = 0$ at $x_0 = 0$ and detected at $x = 100$ downstream.

different. This can be seen in both the spatial particle distributions and the first passage time distributions.

Figure 2 shows average particle densities for the three cases under consideration at a given time. For the distribution dominated scenario (case 1) the density is characterized by a sharp leading edge and a trailing tail, while the correlation-dominated cases (2 and 3) are characterized by forward tails that express fast transport over relatively large distances. The tail obtains more weight with decreasing γ because the frequency of long conduits increases. Correspondingly, the first passage time distributions for the correlation-dominated scenarios, shown in Fig. 3, are characterized by a relatively high frequency of early and low frequency of late arrival. The mean and mean squared first passage time are finite in contrast to the distribution dominated case, for which $\bar{f}(x, t)$ has a power-law tail at long times.

In conclusion, we have shown that average transport in quenched random velocity fields characterized by arbitrary correlation structure and distribution of point values follows a continuous time random walk. For uncorrelated disorder, space and time increments are uncoupled, while spatial correlation gives rise to coupling. Using this average model we studied anomalous transport caused by power-law disorder distributions and power-law disorder correlations. While the anomalous diffusion behavior can be identical in both cases, the transport mechanisms are fundamentally different as reflected in the spatial particle densities and first passage time distributions.

*marco.dentz@idaea.csic.es

[1] R. Kubo, M. Toda, and N. Hashitsume, *Statistical Physics II, Non-Equilibrium Statistical Mechanics* (Springer Verlag, Berlin, Heidelberg, 1991).

[2] J. P. Bouchaud and A. Georges, Phys. Rep. **195**, 127 (1990).

[3] B. Berkowitz, A. Cortis, M. Dentz, and H. Scher, Rev. Geophys. **44**, RG2003 (2006).

[4] B. Berkowitz and H. Scher, Phys. Rev. Lett. **79**, 4038 (1997).

[5] J. D. Seymour, J. P. Gage, S. L. Codd, and R. Gerlach, Phys. Rev. Lett. **93**, 198103 (2004).

[6] A. M. Tartakovsky, D. M. Tartakovsky, and P. Meakin, Phys. Rev. Lett. **101**, 044502 (2008).

[7] T. Le Borgne, M. Dentz, and J. Carrera, Phys. Rev. Lett. **101**, 090601 (2008).

[8] T. Kosztolowicz, K. Dworecki, and S. Mrowczynski, Phys. Rev. Lett. **94**, 170602 (2005).

[9] P. Barthelemy, J. Bertolotti, and D. S. Wiersma, Nature (London) **453**, 495 (2008).

[10] J. Szymanski and M. Weiss, Phys. Rev. Lett. **103**, 038102 (2009).

[11] S. C. Weber, A. J. Spakowitz, and J. A. Theriot, Phys. Rev. Lett. **104**, 238102 (2010).

[12] V. Tejedor, O. Bénichou, R. Voituriez, S. F. Jungmann, C. Selhuber-Unkel, L. B. Oddershede, and R. Metzler, Biophys. J. **98**, 1364 (2010).

[13] R. Metzler and J. Klafter, Phys. Rep. **339**, 1 (2000).

[14] J. H. Cushman, X. Hu, and T. R. Ginn, J. Stat. Phys. **75**, 859 (1994).

[15] M. Magdziarz, A. Weron, K. Burnecki, and J. Klafter, Phys. Rev. Lett. **103**, 180602 (2009).

[16] J. H. Cushman, D. O'Malley, and M. Park, Phys. Rev. E **79**, 032101 (2009).

[17] H. Risken, *The Fokker-Planck Equation* (Springer, Heidelberg, New York, 1996).

[18] H. Scher and M. Lax, Phys. Rev. B **7**, 4491 (1973).

[19] G. Margolin and B. Berkowitz, Phys. Rev. E **65**, 1 (2002).

[20] M. Dentz, A. Cortis, H. Scher, and B. Berkowitz, Adv. Water Resour. **27**, 155 (2004).

[21] T. Geisel, J. Nierwetberg, and A. Zacherl, Phys. Rev. Lett. **54**, 616 (1985).

[22] G. Zumofen and J. Klafter, Phys. Rev. E **47**, 851 (1993).

4